JOURNAL OF MATERIALS SCIENCE 29 (1994) 6061–6068

Effect of atmosphere on the PTCR properties of $BaTiO_3$ ceramics

D. C. SINCLAIR, A. R. WEST
Chemistry Department, University of Aberdeen, Meston Walk, Aberdeen AB9 2UE, UK

The influence of low-temperature annealing, at $< 360\,^{\circ}C$, in various reducing and oxidizing atmospheres for a series of $BaTiO_3$ ceramics with a positive temperature coefficient of resistance (PTCR) is discussed. Combined impedance and modulus spectroscopy is used to analyse a.c. impedance data and shows that the total resistance of the sample can be composed of up to three components, dependent on the cooling rate from the sintering temperature. For quickly cooled samples the PTCR response is dominated by an outer shell on individuals grains, whereas for slowly cooled samples the grain boundary resistance dominates.Annealing in reducing atmospheres destroys the grain boundary PTCR effect whereas the outer-shell grain PTCR effect is relatively insensitive to the reducing atmosphere. It is proposed that the acceptor states responsible for the outer-grain and grain-boundary PTCR effects are predominantly intrinsic metal vacancies, i.e. Ba and/or Ti, and adsorbed oxygen, respectively.

1. Introduction

The positive temperature coefficient of resistance (PTCR) effect in doped semiconducting $BaTiO_3$ is associated with a dramatic semiconductor-to-insulator transition as the temperature is raised above that of the ferroelectric–paraelectric transition around 120 °C [1–5]. Typically, the resistance increases from $< 100\,\Omega$ to 10^6–$10^9\,\Omega$ over a range of 50–100 °C.

PTCR $BaTiO_3$ ceramics are electrically inhomogeneous. Analysis of a.c. impedance data using impedance and electric modulus spectroscopy presentations has shown that the ceramics usually have at least three electrical components (Fig. 1) [6]. These are first an outer, grain boundary region characterized by resistance R_1 and capacitance C_1. Often resistance R_1 dominates the PTCR response (Fig. 2); C_1 is temperature-independent which indicates that it is due to a non-ferroelectric region of the ceramic. Second, the individual grains appear to have an outer, shell-type thick layer whose resistance R_2 shows a PTCR effect (Fig. 2). These regions are ferroelectric, as shown by their capacitance (C_2) behaviour which obeys the Curie–Weiss law for temperatures above the Curie temperature [7, 8]. This R_2C_2 region is usually termed the bulk response. Third, the grain cores appear to be semiconducting with a resistance (R_3) below T_c of a few ohms. R_3 changes little with temperature and certainly does not show any dramatic PTCR effect. It may actually pass through a shallow minimum at T_c [9, 10]. Nothing is known about C_3 or its temperature dependence.

It is well known that the resistance of PTCR $BaTiO_3$ ceramics demonstrates significant atmosphere dependence in the negative temperature coefficient of resistance (NTCR) region above 250 °C [11, 12]. Typically, the resistance may decrease by several orders of magnitude in reducing atmospheres [13]. Despite the consequent instability in PTCR devices to high-temperature reduction, there have been relatively few investigations into the origin of this atmosphere dependence.

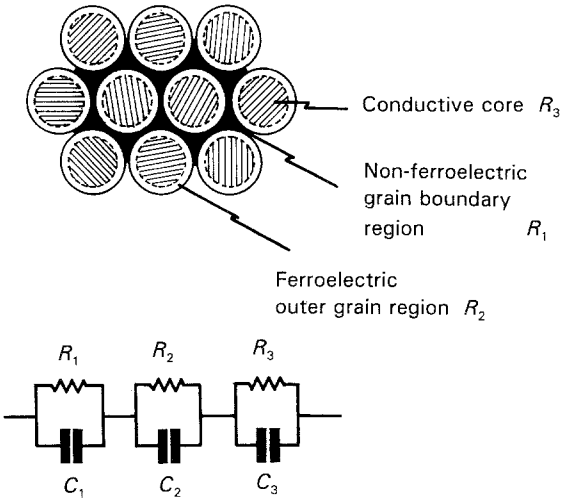

Figure 1 Schematic model of polycrystalline PTCR $BaTiO_3$.

Heywang [2] in his original model to explain the PTCR effect did not consider the nature of the grain-boundary surface states, but instead assumed they were impurities from the raw materials. In the model of Daniels *et al.* [14] the surface states were thought to be barium vacancies, whereas Jonker [15] and Lewis

0022–2461

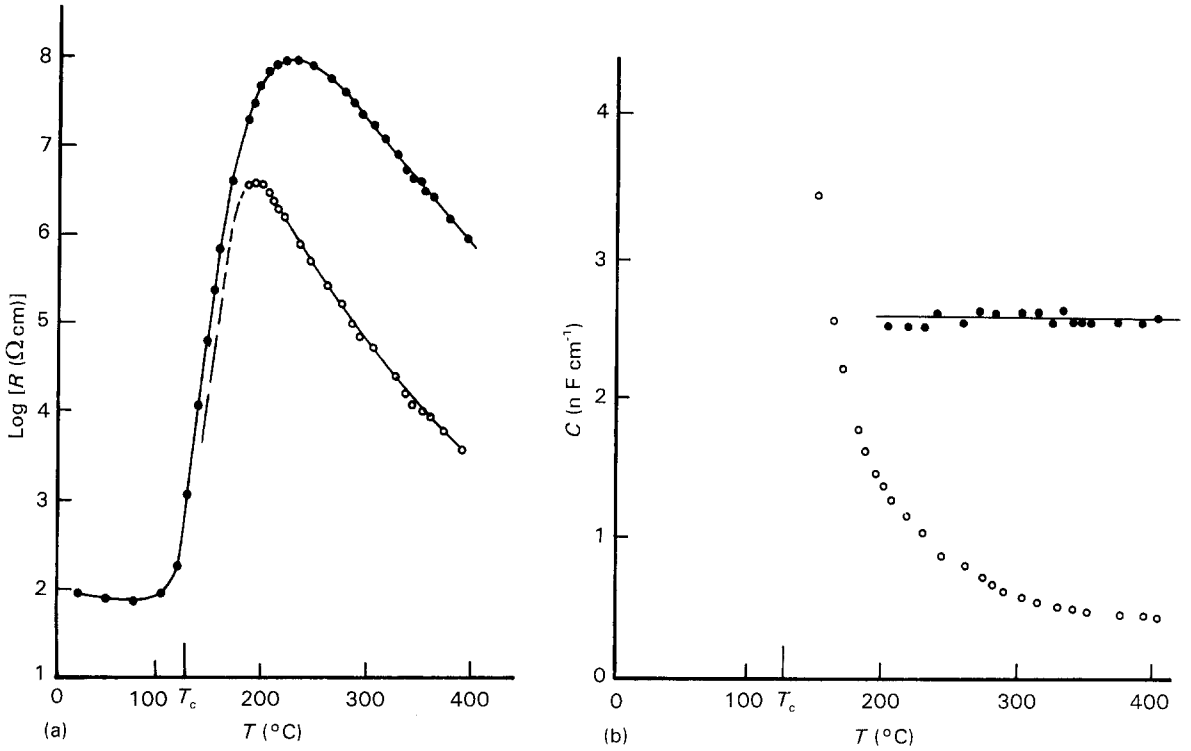

Figure 2 Temperature dependence of resistances (a) R_1 and R_2 and (b) capacitances C_1 and C_2 for sample C: (●) R_1, C_1; (○) R_2, C_2.

and Catlow [16] suggested the presence of adsorbed oxygen. The latter proposal has been supported by the work of Tien and Carlson [17], MaChesney and Potter [18] and Kuwubara *et al.* [12].

The purpose of the present paper is to show, using a.c. impedance techniques, the low-temperature (< 360 °C) atmosphere dependence of the grain-boundary (R_1C_1) and ferroelectric shell-type (R_2C_2) components for various PTCR ceramics. These results are discussed in terms of a core–shell model for PTCR $BaTiO_3$ ceramics.

2. Experimental procedure

The PTCR $BaTiO_3$ ceramics were kindly provided by R.E.W. Casselton of Bowthorpe Thermometrics (Taunton, UK). A series of samples was prepared in which the cooling time from the sintering temperature, 1320 °C, to room temperature was varied systematically from 0.5 (sample A) to 14.5 h (sample G). All other parameters were fixed, i.e. the heating profile and the concentration of donors, acceptors, grain growth inhibitors and sintering aids. Pellets were fired at 1320 °C for 30 min and then cooled to room temperature. Ohmic contacts were then applied to the pellets to produce PTCR devices.

A Solartron 1250/1286 frequency response analyser and electrochemical interface was used for a.c. impedance measurements over the frequency range 30 mHz to 65 kHz. This system was linked to a BBC microcomputer for programming the measurements and for storing and handling the data.

All samples were treated under the same experimental conditions. For a.c. impedance measurements, the electrodes on each sample were attached to the Pt leads of a controlled-atmosphere conductivity jig and heated inside a tube furnace, with temperatures controlled and measured to within 3 °C. A.c. impedance data were recorded between 25 and 360 °C. The atmosphere was initially laboratory air and was then changed sequentially to flowing O_2, N_2 and N_2–NH_3 mixtures, each for a period of 100 h at 355 °C. For each atmosphere, variations in resistance of the various components were monitored first as a function of time at 355 °C and then as a function of temperature between 360 and 25 °C.

After exposing the samples to the conditions described above, each sample was recovered from the conductivity jig, embedded in 2 g of succinic acid, $(CH_2CO_2H)_2$, and heated in a horizontal tube furnace at 350 °C in flowing N_2. Succinic acid decomposes at 267 °C [19] into a mixture of reducing gases, in particular CO, thus creating a strongly reducing atmosphere. After 1 h the samples were cooled to 25 °C in N_2, replaced in the conductivity jig and the a.c. response measured, in N_2, from 25 to 360 °C. If any reduction in the PTCR effect had occurred the atmosphere was subsequently switched to O_2 in an attempt to determine whether the original PTCR effect could be recovered.

3. Results and discussion

Results are presented in Fig. 3 for samples A, C and G, which showed the two extremes (A and G) and optimum (C) behaviour of PTCR $BaTiO_3$ ceramics. Data for samples B and D–F (cooled at intermediate rates) were also obtained. Their electrical properties were intermediate between those of A and G [8]. Thus, the room-temperature resistance R_{25} increased linearly with cooling time (Fig. 3 inset) and the PTCR

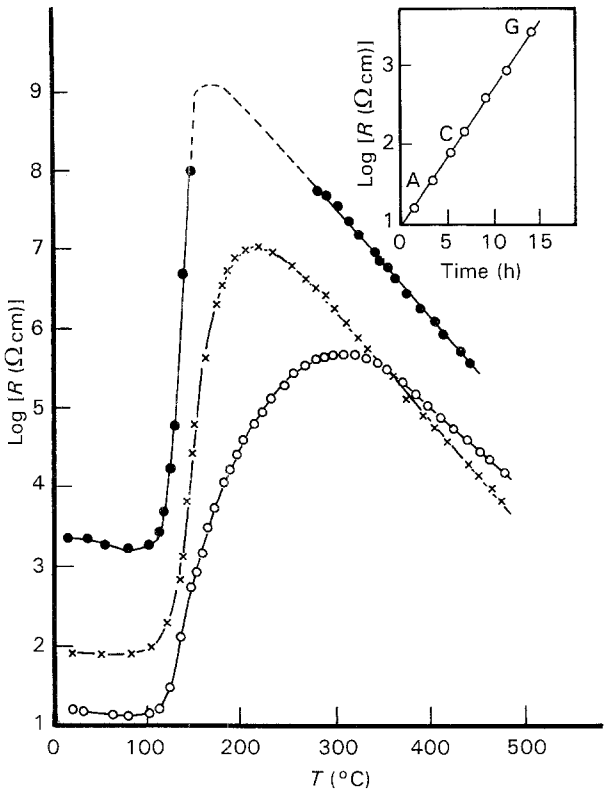

Figure 3 Resistivity against temperature for PTCR $BaTiO_3$ ceramic samples (○) A, (×) C and (●) G. The inset shows the room-temperature (25 °C) resistivity of the ceramics as a function of the time to cool the sample to ambient.

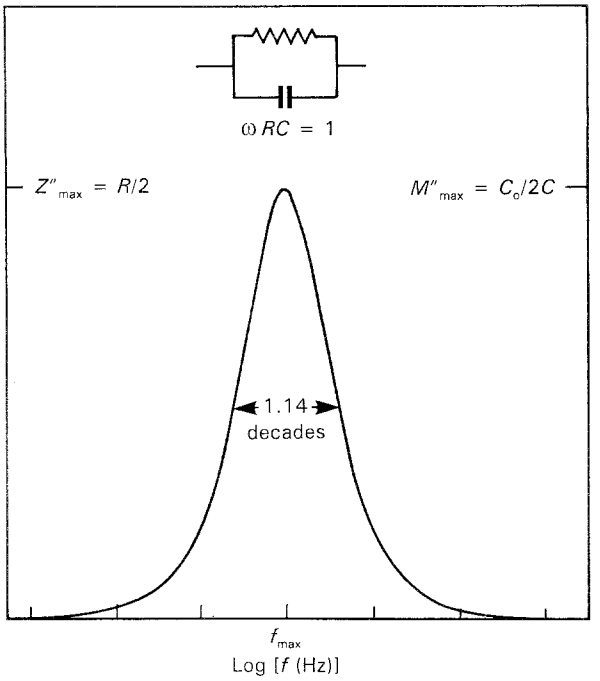

Figure 4 Impedance Z'' and modulus M'' spectroscopic plots against frequency f for the circuit shown.

range (R_{max}/R_{25}), also increased with cooling time. In addition, the sharpness of the resistance rise (the so-called "PTCR action") above T_c generally increased in the sequence A to G.

3.1. Data analysis

Data were initially obtained in the complex impedance notation, i.e. as Z', Z'' at each frequency f. We have shown previously [6] that complex impedance plane plots of Z'' versus Z' are useful for determining the dominant resistance of a sample (usually R_1) but are insensitive to smaller resistances. Instead, a much more useful analysis is to present data as combined impedance (Z'') and modulus (M'') spectroscopic plots (i.e. against frequency). These plots are related as follows.

For the parallel RC circuit shown in Fig. 4, it can be readily shown that

$$Z'' = R\left(\frac{\omega RC}{1+(\omega RC)^2}\right) \quad (1)$$

$$M'' = \frac{C_0}{C}\left(\frac{\omega RC}{1+(\omega RC)^2}\right) \quad (2)$$

where $\pi = 2\pi f$ is the angular frequency and C_0 the vacuum capacitance of the cell. The term in large brackets is the same for Z'' and M'' and gives the Debye-like peak shape in the spectroscopic plots of Fig. 4. The peak heights are proportional to R for the Z'' peak and to C^{-1} for the M'' peak. Hence the power of combined impedance and modulus spectroscopy is that the Z'' plot highlights phenomena with the largest resistance whereas M'' picks out those of the smallest capacitance.

A typical Z'', M'' plot for PTCR sample G is shown in Fig. 5. It shows a single Z'' peak of almost ideal shape with a width at half height of 1.20 decades (ideal theoretical value = 1.14 decades). The M'' spectrum shows a small peak coincident in frequency with the Z'' peak and, at higher frequencies, a much larger, broad/doubled peak. This has a small associated resistance since the Z'' value is low at these frequencies, but nevertheless it represents the main volume fraction (within the measurable frequency range available) of the sample* since it has a much smaller capacitance than the lower-frequency peak which dominates the Z'' spectrum.

Plots such as Fig. 5 may be used as a very convenient visual monitor of the electrical make-up of the sample and provide a useful means to show the effect of changing conditions, i.e. temperature and/or atmosphere. There are three key points that may be used as a fingerprint test:

(a) the peak height of the Z'' peak, which is proportional to R;

(b) the height of the M'' peak, which is proportional to C^{-1}; and

* Accurate estimates of the volume fraction of different regions of a sample would require knowledge of (a) their individual geometry–thickness, area, orientation–and (b) their individual permittivity. We have no direct knowledge of either of these factors. For the present purposes, in making qualitative assessments we assume that the permittivities are approximately equal and the geometrical shapes of the regions are similar; differences in capacitance can then be related to differences in volume fraction.

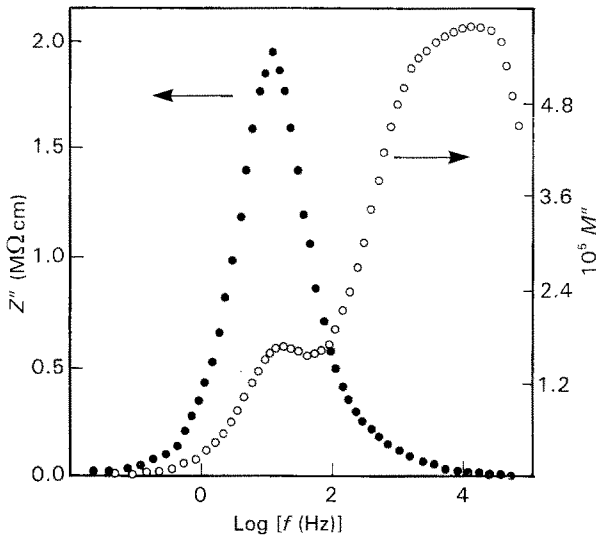

Figure 5 (●) Impedance Z'' and (○) modulus M'' spectroscopic plots versus log (frequency) for sample G at 355 °C.

(c) the frequency of the peak maxima (in both Z'' and M'') since the relation

$$\omega RC = 1 \quad (3)$$

holds at the peak maximum.

Thus for instance, in the case of the M'' peak, a shift in f_{max} at constant M''_{max} would imply variation in R but not in C. If instead there was a change in the M''_{max} value but no variation in f_{max}, then both R and C would have changed.

For the present materials, an increase in sample resistance may be associated with an increase in the acceptor concentration, leading to an increase in either the resistivity or the volume fraction of a particular region within the sample. If an increase in R is due only to an increase in resistivity, the associated M''_{max} value should remain unchanged. If instead there is an increase in volume fraction, the M''_{max} value should increase as the associated capacitance decreases; since the associated resistance would also increase, f_{max} of the M'' peak should remain constant. Thus combined Z'', M'' spectroscopy allows us to distinguish whether a change in sample resistance is associated with a change in resistivity or with a variation in volume fraction.

The results obtained depended very much on whether the PTCR pellet exhibited the grain boundary resistance R_1 (not present in A, present in C and G) as well as the shell resistance R_2 (present in all samples). For this reason the atmosphere dependences of these two types of sample are considered individually.

3.2. Sample A

The resistance of this sample (R_2) and its PTCR range were insensitive to both oxidizing and reducing (mild and strong) atmospheres at 355 °C. No change was observed in the combined Z'', M'' spectroscopic plots. Thus, the ferroelectric shell-type regions (R_2) could not be reduced nor the grain boundary component oxidized from the various atmospheres employed at 355 °C. The insensitivity of the ferroelectric shell-type regions to the oxygen partial pressure at 355 °C is strong evidence that these layers consist of "frozen-in" metal vacancies, i.e. Ba and/or Ti. These vacancies act as electron traps [4] and are primarily responsible for the observed PTCR effect in this sample.

The poor PTCR range and shallow PTCR action of quickly cooled samples such as sample A (Fig. 3) can be explained by the fact that the grain boundary component R_1 is more conductive than that of the ferroelectric shell-type regions R_2. This can be attributed to the presence of donor-type oxygen vacancies in the grain boundaries as has been suggested previously [16]. For such an oxygen vacancy model, it is expected that the grain boundary resistance R_1 would exhibit O_2 sensitivity.

There cannot have been a large adsorption of O_2 on annealing in oxygen at 355 °C, since the adsorbed molecules would have filled the oxygen vacancies according to the reaction

$$V_{\ddot{O}} + O_2 \rightarrow O_O^X + 2\dot{h} \quad (4)$$

thus leading to a substantial increase in the grain boundary resistance. The absence of any O_2 dependence does not imply that O_2 was not adsorbed by the sample, but rather that it was insufficient to increase the grain boundary resistance R_1 to a detectable level.

3.3. Samples C and G

Sample C represents a PTCR device commonly employed for industrial applications. A good PTCR range, i.e. a small R_{25} and a large R_{max}, was obtained from the intermediate cooling time employed during the post-sintering process. The grain boundary resistance R_1 dominates the PTCR range, with a second, smaller PTCR effect, R_2 (Fig. 2) attributable to the ferroelectric shell-type regions. The grain boundary component is attributed primarily to the filling of donor-type oxygen vacancies by adsorbed oxygen during cooling, as given by Equation 4.

Sample G represents a PTCR device in which both R_{25} and R_{max} are large and thus the PTCR effect is dominated by the grain boundary component R_1. The substantial increase in the values of R_{25} and R_{max} of sample G (Fig. 3) is attributed to the large concentration of adsorbed oxygen (i.e. acceptor states) at the grain boundaries due to the slow cooling time.

The atmosphere-dependent behaviours of samples C and G are discussed together.

3.3.1. Oxidizing and mildly reducing atmosphere effects

Fig. 6 demonstrates the slow increase and decrease in total resistance at 355 °C of sample G for oxidizing and mildly reducing atmospheres, respectively. The resistance values were obtained from the low-frequency intercept of the complex impedance plane plots and correspond to the d.c. resistance of the sample. Changes in resistance of the various components in different atmospheres were most effectively determined by monitoring the variations, if any, in f_{max}

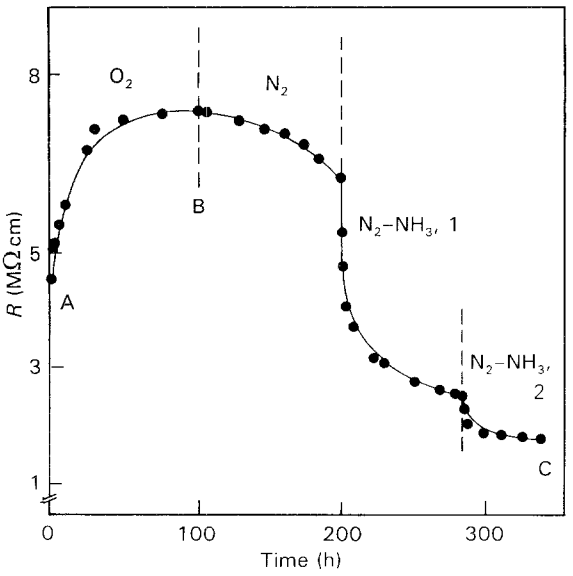

Figure 6 Variation of total resistance with time for sample G in various atmospheres at 355 °C.

values and the heights of the Z'' and M'' spectroscopic peaks, as discussed in Section 3.1.

The results at 355 °C for both samples may be summarized as follows.

(i) The Z'' peak, attributed to the resistive grain boundary component, changed in both height and f_{max} value in the various atmospheres. In oxygen, the Z'' peak height increased and the f_{max} value decreased, whereas in reducing atmospheres the peak height decreased and f_{max} increased (Fig. 7).

(ii) The low-frequency M'' peak, attributed also to the grain boundary component, (Fig. 5) demonstrated small variations in f_{max} for the different atmospheres, with no significant changes in magnitude: the f_{max} value increased in reducing atmospheres and decreased in oxidizing atmospheres.

(iii) The high-frequency M'' peak, attributed to the less resistive ferroelectric shell-type component, was unchanged in both magnitude and f_{max} value for the various atmospheres.

From the above observations, the grain boundary component R_1 was established to be atmosphere-sensitive (points (i) and (ii)) whereas the ferroelectric shell-type component was insensitive to these mild variations in atmosphere (point (iii)). Since there was no change in magnitude of the grain boundary M'' response (point (ii)), the variation in grain boundary resistance may be attributed to a change in acceptor-state concentration rather than a change in volume fraction, i.e. to adsorption and desorption of oxygen from the grain boundary regions. For such mildly reducing atmosphere there was no significant change in the overall PTCR profile of either sample C or G.

The increasing sensitivity of samples A, C and G to mild changes in reducing atmospheres can be attributed to desorption of oxygen from the grain boundary regions. Thus, as the grain boundary resistance increases to dominate the overall sample resistance (samples B to G) the sensitivity of the PTCR device to atmosphere also increases.

3.3.2. *Strongly reducing atmospheres: succinic acid treatment*

The PTCR effect of both samples was changed substantially by heating in a strongly reducing atmosphere, as shown for sample G in Fig. 8. R_{25} was

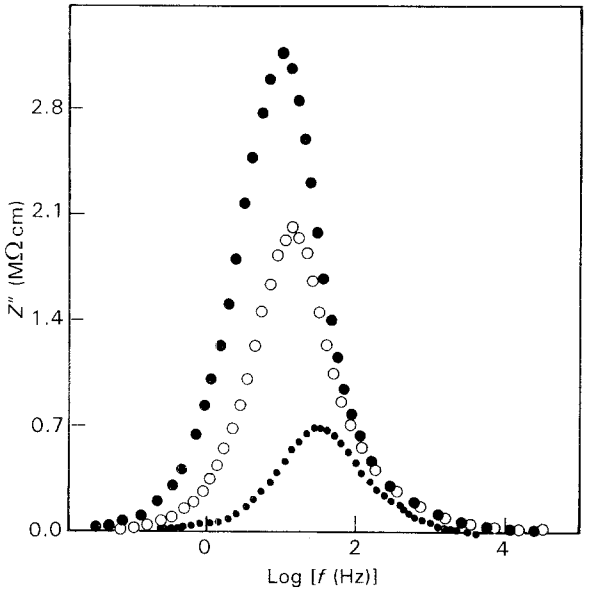

Figure 7 Variation in Z'' spectroscopic plots for sample G in different atmospheres at 355 °C: (○) air, (●) O_2, (◐) N_2–NH_3.

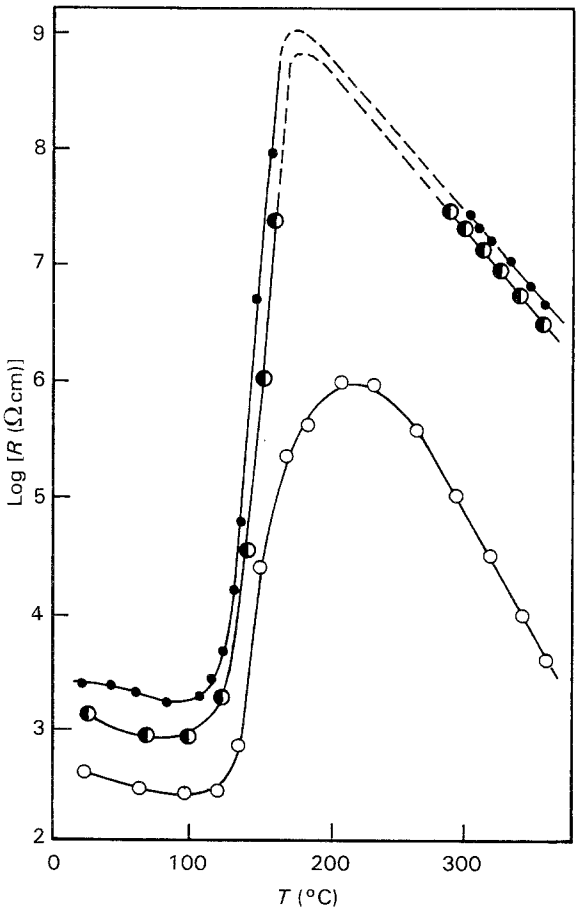

Figure 8 (●) PTCR effect for sample G equilibrated in air at 355 °C, (○) reduction of the effect after succinic acid treatment at 350 °C, (◐) subsequent recovery in O_2 at 355 °C.

reduced from 2300 to 490 Ω cm, R_{max} to ~ 1 MΩ cm and the PTCR range to ~ 3.5 orders of magnitude. It appears also that T_{max} increased to 220 °C.

In the temperature range between 150 and 310 °C on the heating cycle (in flowing N_2 to suppress re-oxidation) the Z'' and M'' spectra (not shown) consisted of single, broad peaks; the M'' peak height increased with temperature and the f_{max} values of Z'' and M'' peaks were very similar. The sample resistance at 355 °C was small and the f_{max} values of the Z'' and M'' spectra in excess of 65 kHz. From the limited data available, it appeared that the sample resistance was dominated by the ferroelectric shell-type component.

To determine whether the reduction was reversible and if so how long it would take for the various regions to regain their original values, the atmosphere was changed from N_2 to O_2, at 355 °C. After 200 h of re-oxidation, the total resistance had increased from 600 Ω cm to a value approaching that of the air-equilibrated value, 3.5 MΩ cm (Fig. 9 inset). The PTCR effect was reversible after the succinic acid treatment, therefore, provided the sample was annealed in O_2 for long periods of time, > 200 h, at 355 °C (Fig. 8).

Modulus and impedance data were analysed at 355 °C to determine if the recovery in total resistance with time could be separated into the component resistances. The complex impedance plane plots consisted of two overlappping semi-circular arcs (Fig. 10). The lower-frequency arc was attributed to the grain boundary response (R_1) and the higher-frequency arc to the impedance of the ferroelectric shell-type regions (R_2). The variations in these plots could be summarized as follows:

(i) For short re-oxidation periods, i.e. < 12 h the impedance of the ferroelectric shell-type regions dominated the sample resistance (Fig. 10a).

(ii) After 12 h of re-oxidation, the grain boundary impedance was comparable to that of the ferroelectric shell-type regions (Fig. 10b).

(iii) For re-oxidation periods in excess of 12 h the grain boundary component dominated the overall sample impedance (Fig. 10c).

The variation in resistance of these components with re-oxidation time at 355 °C is summarized on Fig. 9. The combined resistance of the ferroelectric shell-type layers (filled squares) initially dominates the total sample resistance (filled circles). The grain boundary resistance (open circles), however, rises rapidly on re-oxidation. After 24 h it dominates the sample resistance, as the resistance of the ferroelectric shell-type regions approaches a constant value at 355 °C.

Combined M'' spectroscopic plots are shown in Fig. 11 for various re-oxidation times. For comparison, an ideal Debye peak (solid line) has been included in this diagram. For short re-oxidation periods the similarity in time constants of the elements present results in broad and non-Debye-like M'' spectra. For long re-oxidation periods (Fig. 11 spectrum 3) improved resolution of the M'' peaks is obtained as the grain boundary component dominates the sample resistance. This last spectrum is similar to the air-equilibrated response at 355 °C before any atmosphere treatment (Fig. 5). Furthermore, the broadness of the high-frequency M'' peak demonstrates the inhomogeneous nature of the ferroelectric shell-type regions.

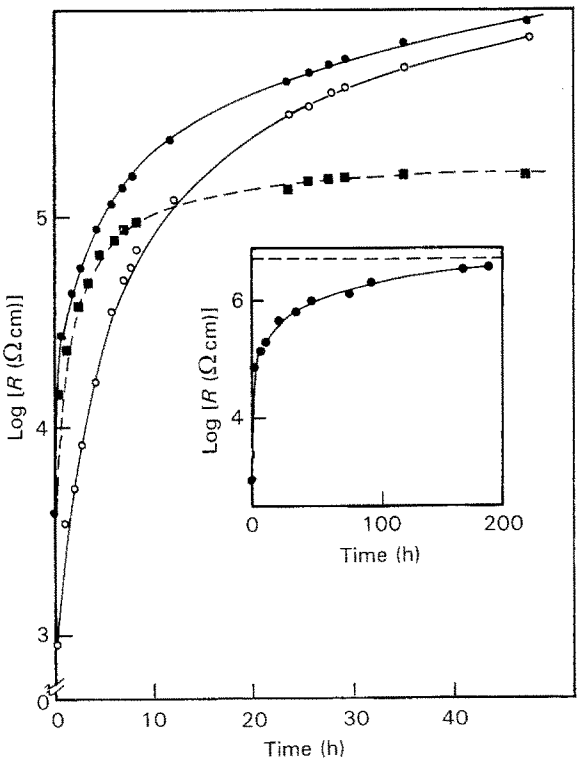

Figure 9 Recovery of component resistances for sample G in O_2 at 355 °C, after succinic acid treatment: (○) R_1 (grain boundary), (■) R_2 (bulk), (●) $R_T = R_1 + R_2$. Inset: (●) increase in total resistance for long re-oxidation periods, (– –) as-received total resistance at 355 °C before succinic acid treatment.

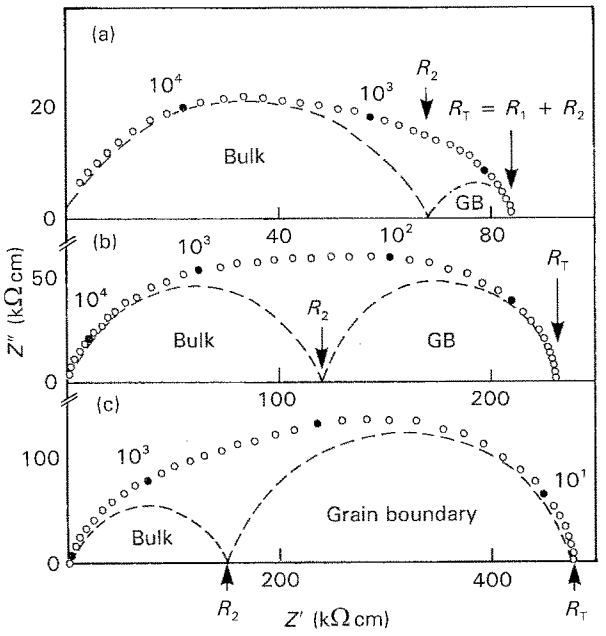

Figure 10 Complex impedance plane plots for sample G after re-oxidation periods of (a) 4.5, (b) 12 and (c) 25.5 h at 355 °C.

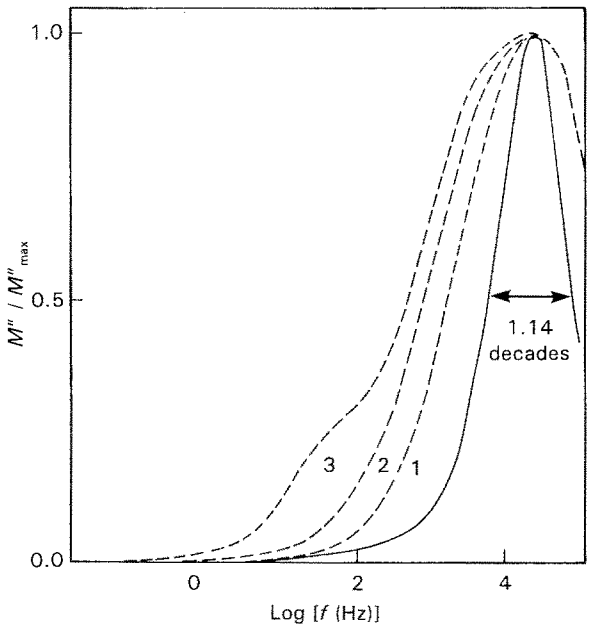

Figure 11 Normalised M'' spectroscopic plots for sample G at 355 °C after re-oxidation periods of (1) 4, (2) 20 and (3) 189 h. An ideal Debye peak, (——), is included for comparison with the experimental data.

Unlike the M'' spectra, where the f_{max} of the high-frequency M'' peak displayed small variations with re-oxidation time, the f_{max} values of the Z'' peak demonstrated significant time dependence. As the sample resistance increased the f_{max} of the Z'' peak decreased, from > 65 kHz to 12 Hz.

The PTCR behaviour of sample G on reduction in succinic acid and re-oxidation in O_2 appears quite clear. On reduction,both components which give rise to the PTCR effect in sample G have smaller resistances. The small PTCR effect that remains is due primarily to the ferroelectric shell-type regions. The grain boundary resistance has been reduced, due to desorption of O_2, thus creating donor-type oxygen vacancies in both the grain boundaries and ferroelectric shell-type regions. On re-oxidation, however, as oxygen is adsorbed, thus annihilating the oxygen vacancies created during reduction, the grain boundary resistance increases rapidly (Fig. 9). For long re-oxidation times, i.e. > 200 h at 355 °C, the sample resistance is nearly re-established (Fig. 9 inset). Furthermore the PTCR effect, which is dominated by the grain boundary component, is also recovered (Fig. 8c).

The electrical response of sample C on reduction in succinic acid was similar to that of sample G, in that the resistance of both the grain boundary and ferroelectric shell-type regions was reduced. Re-oxidation at 355 °C showed that although the grain boundary component dominated the sample resistance after long re-oxidation periods, the sample resistance after short times was predominantly that of the ferroelectric shell-type regions. Thus, in samples C and G the post-reduction PTCR effect was attributed to the ferroelectric shell-type regions.

The reduction of the ferroelectric shell-type regions in samples C and G must be related to the presence of a resistive atmosphere-sensitive grain boundary component. A plausible explanation may be that on reduction of the grain boundary component, oxygen vacancies are created at the grain boundaries and penetrate the ferroelectric shell type regions as they diffuse into the core of the grains, in an attempt to establish equilibrium throughout the sample. The presence of such donors would reduce the resistance of the ferroelectric layer regions and account for the observed behaviour.

4. Summary

Heat treatment in an atmosphere of decomposing succinic acid gave a quick and effective method with which to test the sensitivity of PTCR devices, prepared under various cooling conditions, to reducing atmospheres. Sample A was insensitive to this treatment, whereas the PTCR effects of samples C and G were substantially diminished. There is clearly a major difference between sample A and samples C and G. Although all samples were electrically inhomogeneous, the PTCR effects of samples C and G were dominated by a grain boundary component (R_1C_1) whereas sample A was dominated by the ferroelectric shell-type (R_2C_2) component. Furthermore, the PTCR effect of sample A was smaller than that of C or G, both of which exhibited PTCR "ranges" in excess of six orders of magnitude.

Since sample A was insensitive to the strong reduction, it is proposed that the large reduction in the PTCR effect observed in samples C and G is due primarily to the decrease in resistance of the grain boundary component. The a.c. impedance results give conclusive evidence for this process. The ferroelectric shell-type regions for samples C and G are also reduced, but to a much smaller extent. After long periods of oxidation, i.e. > 200 h, the PTCR effect of the samples was fully recovered.

In accordance with other workers [12, 15–18], the reduction and re-oxidation of the grain boundary component is attributed to the desorption and adsorption of O_2 at the grain boundaries, respectively. The behaviour of the ferroelectric shell-type regions with variations in gas atmosphere is more complicated. For sample A, the associated resistance values were insensitive to both mild and strongly reducing atmospheres at 355 °C, whereas for samples C and G the associated resistance values were diminished in strongly reducing atmospheres. The precise nature of the acceptor states in these regions is unknown, but they are proposed to consist mainly of intrinsic metal vacancies, as first suggested by Daniels *et al.* [14]. The reason why these regions are insensitive to reduction for quickly cooled samples (sample A) but are sensitive for more slowly cooled samples (samples C and G) remains unclear.

References

1. O. SABURI, *J. Phys. Soc. Jpn.* **14** (1959) 1159.
2. W. HEYWANG, *J. Mater. Sci.* **6** (1971) 1214.
3. G. H. JONKER, *Solid State Electron.* **7** (1964) 895.

4. J. DANIELS and R. WERNIKE, *Philips Res. Rep.* **31** (1976) 544.
5. T. R. N. KUTTY, P. MURUGARAJ and N. S. GAJBHIYE, *Mater. Res. Bull.* **20** (1985) 565.
6. D. C. SINCLAIR and A. R. WEST, *J. Appl. Phys.* **66** (1989) 3850.
7. *Idem, J. Mater. Sci. Lett.* **7** (1988) 823.
8. *Idem*, "Surfaces and Interfaces of Ceramic Materials" (Kluwer, 1989) p. 535.
9. T. Y. TSENG and S. H. WANG, *Mater. Lett.* **9** (1990) 164.
10. D. E. JOHNSTON, D. C. SINCLAIR and A. R. WEST, "Special Ceramics 9", British Ceramic Proceedings (1991) p. 223.
11. I. UEDA and K. IKEGAMI, *J. Phys. Soc. Jpn* **20** (1965) 546.
12. M. KUWUBARA, S. SUEMURA and M. KAWAHARA, *Amer. Ceram. Soc. Bull.* **64** (1985) 1394.
13. M. KUWUBARA and T. IDE, *ibid.* **66** (1987) 1401.
14. J. DANIELS, K. K. HARDTL, D. HENNINGS and R. WERNIKE, *Philips Res. Rep.* **31** (1976) 487.
15. G. H. JONKER, *Mater. Res. Bull.* **2** (1987) 401.
16. G. V. LEWIS and C. R. A. CATLOW, *J. Amer. Ceram. Soc.* **68** (1985) 555.
17. T. Y. TIEN and W. G. CARLSON, *ibid.* **46** (1983) 297.
18. J. B. MaCHESNEY and J. F. POTTER, *ibid.* **48** (1965) 81.
19. R. C. WEAST (ed.), "Handbook of Physics and Chemistry", 55th Edn (1974) p. C495.

Received 14 April
and accepted 16 May 1994